Inorg. Chem. **2003**, *42*, 1538−1548

The Arrangement of First- and Second-Shell Water Molecules in Trivalent Aluminum Complexes: Results from Density Functional Theory and Structural Crystallography

Charles W. Bock,[†,‡] George D. Markham,[†] Amy K. Katz,[†] and Jenny P. Glusker*[,†]

Philadelphia University, Henry Avenue and Schoolhouse Lane, Philadelphia, Pennsylvania 19144, and Institute for Cancer Research, Fox Chase Cancer Center, 7701 Burholme Avenue, Philadelphia, Pennsylvania 19111

Received October 7, 2002

The structural and energetic features of a variety of gas-phase aluminum ion hydrates containing up to 18 water molecules have been studied computationally using density functional theory. Comparisons are made with experimental data from neutron diffraction studies of aluminum-containing crystal structures listed in the Cambridge Structural Database. Computational studies indicate that the hexahydrated structure $Al[H_2O]_6^{3+}$ (with symmetry T_h), in which all six water molecules are located in the innermost coordination shell, is lower in energy than that of $Al[H_2O]_5^{3+}\cdot[H_2O]$, where only five water molecules are in the inner shell and one water molecule is in the second shell. The analogous complex with four water molecules in the inner shell and two in the outer shell undergoes spontaneous proton transfer during the optimization to give $\{Al[H_2O]_2[OH]_2\}^{+}\cdot[H_3O^+]_2$, which is lower in energy than $Al[H_2O]_6^{3+}$; this finding of H_3O^+ is consistent with the acidity of concentrated Al^{3+} solutions. Since, however, $Al[H_2O]_6^{3+}$ is detected in solutions of Al^{3+}, additional water molecules are presumed to stabilize the hexa-aquo Al^{3+} cation. Three models of a trivalent aluminum ion complex surrounded by a total of 18 water molecules arranged in a first shell containing 6 water molecules and a second shell of 12 water molecules are discussed. We find that a model with S_6 symmetry for which the $Al[H_2O]_6^{3+}$ unit remains essentially octahedral and participates in an integrated hydrogen bonded network with the 12 outer-shell water molecules is lowest in energy. Interactions between the 12 second-shell water molecules and the trivalent aluminum ion in $Al[H_2O]_6^{3+}$ do not appear to be sufficiently strong to orient the dipole moments of these second-shell water molecules toward the Al^{3+} ion.

Introduction

Aluminum is the most abundant metallic element on the earth's crust and the third most common element (after oxygen and silicon).[1] It is mainly found in rocks as oxides or aluminosilicates and has not, to date, played a significant role in biological processes. There have been reports of acid rain affecting the extent to which aluminum is leached from rocks and accumulates in the world's water supplies.[2] Studies of dialysis patients with elevated aluminum levels suggest that problems with bones are common as are some forms of dementia.[3] Indeed, aluminum has been reported in elevated levels in the brains of Alzheimer's disease patients. It is not clear, however, whether aluminum is a cause of the formation of abnormal neurofibrillary tangles in the brain, or whether it simply binds to them.[4] As a result of such observations, care in cooking with aluminum pans and in using antacids and deodorants has been recommended by watchdog groups.

Trivalent aluminum ions have a high charge (+3e) and small ionic radius (0.53 Å for coordination number 4, 0.68 Å for coordination number 6).[5] Because the exchange of water around the hydrated aluminum ion with bulk solvent is slow (much slower than most cations), it has been possible to determine the number of water molecules in the inner

* To whom correspondence should be addressed. E-mail: JP_Glusker@fccc.edu. Phone: 215-728-2220. Fax: 215-728-2863.
† Philadelphia University.
‡ Fox Chase Cancer Center.

(1) *The Environmental Chemistry of Aluminum*, 2nd ed.; Sposito, G., Ed.; CRC Lewis Publishers: Boca Raton, FL, 1996.
(2) Martin, R. B. *Acc. Chem. Res.* **1994**, *27*, 204−210
(3) Wills, M. R.; Savory, J. *Lancet* **1983**, *ii*, 29−34.
(4) McLachlan, D. R. C.; Kruck, T. P.; Lukin, W. J.; Krishnan, S. S. *Can. Med. Assoc. J.* **1991**, *145*, 793−804.
(5) Brown, I. D. *Acta Crystallogr.* **1988**, *B44*, 545−553.

10.1021/ic020602e CCC: $25.00
Published on Web 02/01/2003

coordination sphere. Two ^{17}O NMR signals are observed from $H_2{}^{17}O$ in aqueous solutions of Al^{3+} which reflect exchange of coordinated and bulk water on a time scale of seconds.[6] The area under the peaks suggests a hydration number for Al^{3+} of 6; experimental $Al^{3+}-O$ distances for hexahydrated aluminum ions are generally in the range 1.87−1.90 Å.[7]

Calculations on isolated $Al[H_2O]_6{}^{3+}$ complexes have shown that a structure with T_h symmetry is a local minimum on the potential energy surface (PES).[8,9] This structure is such that all the water dipoles are oriented directly toward the highly charged central aluminum ion. The slow ligand exchange rate of aluminum ions combined with their similarity in size to magnesium ions implies that aluminum may inhibit magnesium-utilizing enzymes. The total number of water molecules that comprise the second hydration shell around Al^{3+} is not yet clearly established.[7] With an inner-shell coordination number of 6, there are expected to be 12 water molecules attached by hydrogen bonds to the six inner sphere water molecules around the aluminum ion. Recently, however, a molecular dynamics study by Martinez et al.[10] found a second-shell coordination number of 14, and X-ray diffraction studies have found coordination numbers in the range 12−14.[7]

The present work explores the structures and binding enthalpies of a variety of gas-phase trivalent aluminum complexes containing up to 18 water molecules. The relatively weak hydrogen bonding between water molecules in these complexes, in conjunction with the large electrostatic ion−water interaction, provides a formidable problem for computational studies. We have used density functional theory (DFT) with large basis sets in this investigation. Comparisons of results are made with data from neutron diffraction studies on water organization around aluminum ions in crystal structures listed in the Cambridge Structural Database (CSD).[11]

Computational Methods

The complexes that we studied by computational methods include $Al[H_2O]^{3+}$, $Al[H_2O]_2{}^{3+}$, $Al[H_2O]_4{}^{3+}\cdot[H_2O]_2$, $Al[H_2O]_5{}^{3+}\cdot[H_2O]$, $Al[H_2O]_6{}^{3+}$, $Al[H_2O]_6{}^{3+}\cdot[H_2O]$, and $Al[H_2O]_6{}^{3+}\cdot[H_2O]_{12}$; in some cases, the corresponding mono- and divalent aluminum complexes were also studied for comparison. Optimizations and frequency analyses were performed using the GAUSSIAN 94[12] and 98[13] series of programs with density functional theory (DFT) at the B3LYP/6-31+G** computational level;[14,15] for the smaller complexes, DFT optimizations were carried out with much larger basis sets such as 6-311++G**, 6-311++G(2d,2p), and 6-311++(3df,3pd) using a variety of functionals, as well as with second-order Møller−Plesset (MP2) perturbation theory[16] in order to compare different methodologies.[17,18] Atomic charges were calculated from natural population analyses (NPA), and wave functions were analyzed using natural bond orbitals.[19−21]

Cambridge Structural Database Analyses. The Cambridge Structural Database (CSD, April 2001 version)[11] was searched for all published crystal structures studied by neutron diffraction containing aluminum and water; for comparison, we also searched for the corresponding magnesium compounds in view of our earlier studies.[22] The structures identified in this way were bis(hydrogen maleate) hexa-aqua-magnesium (CIRVAA01),[23] methylammonium aluminum sulfate dodecahydrate alum (MAMALM02),[24] bis(hexa-aqua-aluminum) benzene-hexacarboxylate tetrahydrate (SOGGEA),[25] dimethylammonium hexa-aqua-aluminum disulfate (TAPBOB01),[26] and the neodymium and aluminum complex $[Nd(AlMe_4)_3]\cdot 0.5Al_2Me_6$ (YOSYAG01).[27] The last of these five was not investigated further by us because it contained two metal ions. In addition, the neutron diffraction structure of aluminum chloride hexahydrate[28,29] was included in our study. Because the data were obtained by neutron diffraction, hydrogen atoms in the water molecules were well defined. The program Quest3D that is

(6) Fiat, D.; Connick, R. E. *J. Am. Chem. Soc.* **1968**, *90*, 608−615.
(7) Ohtaki, H.; Radnai, T. *Chem. Rev.* **1995**, *93*, 1157−1204.
(8) Wasserman, E.; Rustad, J. R.; Xantheas, S. S. *J. Chem. Phys.* **1997**, *106*, 9769−9780.
(9) Rudolph, W. W.; Mason, R.; Pye, C. C. *Phys. Chem. Chem. Phys.* **2000**, *2*, 5030−5040.
(10) Martinez, J. M.; Pappalardo, R. R.; Marcos, E. S. *J. Am. Chem. Soc.* **1999**, *121*, 3175−3184.
(11) Allen, F. H.; Bellard, S.; Brice, M. D.; Cartwright, B. A.; Doubleday, A.; Higgs, H.; Hummelink, T.; Hummelink-Peters, B. G.; Kennard, O.; Motherwell, W. D. S.; Rodgers, J. R.; Watson, D. G. *Acta Crystallogr.* **1979**, *B35*, 2331−2339
(12) Frisch, M. J.; Trucks, G. W.; Schlegel, H. B.; Gill, P. M. W.; Johnson, B. G.; Robb, M. A.; Cheeseman, J. R.; Keith, T.; Petersson, G. A.; Montgomery, J. A.; Raghavachari, K.; Al-Laham, M. A.; Zakrzewski, V. G.; Ortiz, J. V.; Foresman, J. B.; Cioslowski, J.; Stefanov, B. B.; Nanayakkara, A.; Challacombe, M.; Peng, C. Y.; Ayala, P. Y.; Chen, W.; Wong, M. W.; Andres, J. L.; Replogle, E. S.; Gomperts, R.; Martin, R. L.; Fox, D. J.; Binkley, J. S.; Defrees, D. J.; Baker, J.; Stewart, J. P.; Head-Gordon, M.; Gonzalez, C.; Pople, J. A. *Gaussian 94*, revision A.1; Gaussian, Inc.: Pittsburgh, PA, 1995.
(13) Frisch, M. J.; Trucks, G. W.; Schlegel, H. B.; Scuseria, G. E.; Robb, M. A.; Cheeseman, J. R.; Zakrzewski, V. G.; Montgomery, J. A., Jr.; Stratmann, R. E.; Burant, J. C.; Dapprich, S.; Millam, J. M.; Daniels, A. D.; Kudin, K. N.; Strain, M. C.; Farkas, O.; Tomasi, J.; Barone, V.; Cossi, M.; Cammi, R.; Mennucci, B.; Pomelli, C.; Adamo, C.; Clifford, S.; Ochterski, J.; Petersson, G. A.; Ayala, P. Y.; Cui, Q.; Morokuma, K.; Malick, D. K.; Rabuck, A. D.; Raghavachari, K.; Foresman, J. B.; Cioslowski, J.; Ortiz, J. V.; Stefanov, B. B.; Liu, G.; Liashenko, A.; Piskorz, P.; Komaromi, I.; Gomperts, R.; Martin, R. L.; Fox, D. J.; Keith, T.; Al-Laham, M. A.; Peng, C. Y.; Nanayakkara, A.; Gonzalez, C.; Challacombe, M.; Gill, P. M. W.; Johnson, B. G.; Chen, W.; Wong, M. W.; Andres, J. L.; Head-Gordon, M.; Replogle, E. S.; Pople, J. A. *Gaussian 98*, revision A.1; Gaussian, Inc.: Pittsburgh, PA, 1998.
(14) Hariharan, P. C.; Pople, J. A. *Theor. Chim. Acta* **1973**, *28*, 213−222.
(15) Becke, A. D. *J. Chem. Phys.* **1993**, *98*, 5648−5652.
(16) Møller, C.; Plesset, M. A. *Phys. Rev.* **1934**, *46*, 618−622.
(17) Johnson, B. G.; Gill, P. M. W.; Pople, J. A. *J. Chem. Phys.* **1993**, *98*, 5612−5626.
(18) Pople, J. A.; Headgordon, M.; Raghavachari, K. *J. Chem. Phys.* **1987**, *87*, 5968−5975.
(19) Reed, A. E.; Curtiss, L. A.; Weinhold, F. *Chem. Rev.* **1988**, *88*, 899−926.
(20) Reed, A. E.; Weinstock, R. B.; Weinhold, F. *J. Chem. Phys.* **1985**, *83*, 735−746.
(21) Glendening, E. D.; Reed, A. E.; Carpenter, J. E.; Weinhold, F. *NBO Version 3.1* (*Gaussian 94*, 1995).
(22) Markham, G. D.; Glusker, J. P.; Bock, C. W. *J. Phys. Chem. B* **2002**, *106*, 5118−5134.
(23) Vanhouteghem, V.; Lenstra, A. T. H.; Schweiss, P. *Acta Crystallogr.* **1987**, *B43*, 523−528.
(24) Abdeen, A. M.; Will, G.; Schafer, W.; Kirfel, A.; Bargouth, M. O.; Recker, K.; Weiss, A. *Z. Kristallog.* **1981**, *157*, 147−166. CSD: Refcode MAMALM02.
(25) Robl, C.; Kuhs, W. F. *J. Solid State Chem.* **1991**, *92*, 101−109. CSD: Refcode SOGGEA.
(26) Kazimirov, V. Y.; Sarin, V. A.; Ritter, C.; Shuvalor, L. A. *Kristallografiya* **1999**, *44*, 61−66. CSD: Refcode TAPBOB06.
(27) Klooster, W. T.; Lu, R. S.; Anwander, R.; Evans, W. J.; Koetzle, T. F.; Bau, R. *Angew. Chem., Int. Ed.* **1998**, *37*, 1268−1270. Refcode YOSYAG 01.
(28) Buchanan, D. R.; Harris, P. M. *Acta Crystallogr.* **1968**, *B24*, 953−960.
(29) Andress, K. R.; Carpenter, C. *Z. Kristallogr.* **1934**, *87*, 446−463.

connected with the CSD was used.[11] The structures were viewed by use of the graphics program ICRVIEW,[30] and the metal ion coordination geometry was evaluated for each structure. Analyses of metric details of coordination geometry were done by use of the in-house program BANG.[31] Among crystal structures studied by X-ray diffraction, 37 aluminum-containing structures in the CSD have at least one metal-ion-bound water molecule. Nine crystal structures have been found that contain a hexahydrated aluminum ion.

Results and Discussion

A variety of hydrated Al^{3+} complexes with water molecules in the first and second hydration shells were studied at several computational levels using DFT. The total molecular energies of these complexes are given in Table 1S (Supporting Information). Thermal corrections to 298 K and entropies calculated at the B3LYP/6-31+G**//B3LYP/6-31+G** level are given in Table 2S. A search of the CSD[11] for molecules that contain trivalent aluminum ions reveals that coordination numbers from 4 to 6 are quite common for this metal ion. Before proceeding to hydrates with these higher coordination numbers, and in order to assess effects of various computational methods, we considered the monohydrate $Al[H_2O]^{3+}$.

$Al[H_2O]^{3+}$. We performed a variety of optimizations on the monohydrate $Al[H_2O]^{3+}$ using pure DFT (within the local density approximation (LDA) and the generalized gradient approximation (GGA)), hybrid DFT, Hartree−Fock, and Møller−Plesset perturbative methods in conjunction with several high-quality basis sets. The optimized geometrical parameters are listed in Table 1[15,32−35]; an extensive collection of geometrical parameters for $Al[H_2O]^{3+}$ optimized using HF, MP2, and CCSD(T) methods with correlation consistent basis sets has been given by Wasserman et al.[8] This complex, $Al[H_2O]^{3+}$, which is metastable with respect to the $Al^{2+} + H_2O^+$ asymptote because the second ionization potential (IP) of Al is larger than the first IP of water, is planar with C_{2v} symmetry at all the computational levels we considered.[8] Such a structure is indicative of a strong ion−dipole interaction and is a common feature of many metal ion monohydrates.[36,37] As can be seen from Table 1, the calculated Al−O distance is rather sensitive to the inclusion of multiple polarization functions into the basis set, and the typical 6-311++G** set gives Al−O distances several hundredths of an angstrom unit longer than those found using more complete basis sets for each of the methods we employed. It should be noted that for a given basis set, B3LYP, MP2(FULL), and MP4SDTQ(FULL) give very similar Al−O distances. Among the methods employed (see earlier), LDA gives significantly shorter Al−O distances than does GGA with any of the basis sets that we used.

In Table 2, we compare geometrical parameters and NPA charges for the monohydrates $Al[H_2O]^{n+}$ for $n = 1-3$. As might be expected, when the formal charge on the aluminum ion increases, the Al−O distance decreases, the O−H distances increase, and any transfer of electron density from the water to the cation is increased.[37] Interestingly, one of the B3LYP/6-311++G** NBOs of $Al[H_2O]^{3+}$ is classified as an Al−O bonding orbital;[19−21] it combines the occupied in-plane lone-pair orbital on the water oxygen atom with a 3sp natural hybrid orbital (NHO) on the trivalent aluminum ion (0.23*Al + 0.97*O). There is no corresponding Al−O bonding orbital found in the NBO analyses of either divalent $Al[H_2O]^{2+}$ or monovalent $Al[H_2O]^{1+}$. However, both of the

Table 1. Geometrical Parameters of the Monohydrate $Al[H_2O]^{3+}$ Calculated at Various Computational Levels

computational level	Al−O (Å)	O−H (Å)	∠HOH (deg)
A. Pure DFT			
Local Density Approximation (LDA)[31]			
SVWN5/6-311++G(d,p)	1.751	1.038	107.3
SVWN5/6-311++G(2d,2p)	1.732	1.036	107.4
SVWN5/6-311++G(3df,3pd)	1.726	1.037	107.0
Generalized Gradient Approximation (GGA)[32−34]			
BLYP/6-311++G(d,p)	1.784	1.034	108.5
BLYP/6-311++G(2d,2p)	1.768	1.031	108.6
BLYP/6-311++G(3df,3pd)	1.762	1.032	108.3
B. Hybrid DFT[15]			
B3LYP/6-31+G(d,p)	1.765	1.025	108.1
B3LYP/6-311++G(d,p)	1.762	1.023	107.6
B3LYP/6-311++G(2d,2p)	1.745	1.020	107.8
B3LYP/6-311++G(3df,3pd)	1.739	1.021	107.4
C. Hartree−Fock (HF)			
HF/6-311++G(d,p)	1.737	0.996	106.3
HF/6-311++G(2d,2p)	1.720	0.993	106.6
HF/6-311++G(3df,3pd)	1.716	0.994	106.3
D. Møller−Plesset Perturbation Theory (MP)[16]			
MP2(FULL)/6-311++G(d,p)	1.758	1.016	106.6
MP2(FULL)/6-311++G(2d,2p)	1.741	1.013	107.0
MP2(FULL)/6-311++G(3df,3pd)	1.734	1.014	106.5
MP4SDTQ(FULL)/6-311++G(d,p)	1.761	1.015	106.9
MP4SDTQ(FULL)/6-311++G(2d,2p)	1.743	1.011	107.2
MP4SDTQ(FULL)/6-311++G(3df,3pd)	1.736	1.013	106.7

Table 2. Geometrical Parameters and NPA Charges of the Monohydrates $Al[H_2O]^{n+}$ ($n = 1-3$) Calculated at the MP2(FULL)/6-311++G(3df,3pd)//MP2(FULL)/6-311++G(3df,3pd) {B3LYP/6-31+G(d,p)//B3LYP/6-31+G(d,p)} and [B3LYP/6-311++G(3df,3pd)//B3LYP/6-311++G(3df,3pd)] Computational Levels

	geometrical parameters			NPA charges		
monohydrate	Al−O (Å)	O−H (Å)	∠HOH (deg)	q_{Al}	q_O	q_H
$Al[H_2O]^{1+}$	2.086	0.967	106.6	+0.965e[a]	−1.039e[a]	+0.537e[a]
	{2.125}[b]	{0.975}	{107.4}	{+0.971e}	{−1.130e}	{+0.579e}
	[2.091]	[0.970]	[107.2]	[+0.970e]	[−1.050e]	[+0.540e]
$Al[H_2O]^{2+}$	1.819	0.984	107.0	+1.886e[a]	−1.096e[a]	+0.606e[a]
	{1.851}	{0.992}	{108.0}	{+1.873e}	{−1.173e}	{+0.609e}
	[1.824]	[0.988]	[107.7]	[+1.881e]	[−1.098e]	[+0.609e]
$Al[H_2O]^{3+}$	1.734	1.014	106.5	+2.844e[a]	−1.183e[a]	+0.670e[a]
	{1.765}	{1.025}	{108.1}	{+2.805e}	{−1.246e}	{+0.721e}
	[1.739]	[1.021]	[107.4]	[+2.827e]	[−1.179e]	[+0.676e]

[a] MP2 density. [b] In this and in following tables, brackets and braces indicate the computational level at which these values were calculated.

(30) Erlebacher, J.; Carrell, H. L. *ICRVIEW−Graphics program for use on Silicon Graphics computers;* The Institute for Cancer Research, Fox Chase Cancer Center: Philadelphia, PA, 1992.
(31) Carrell, H. L. *BANG−Molecular geometry program*; The Institute for Cancer Research, Fox Chase Cancer Center: Philadelphia, PA 1976.
(32) Vosko, S. H.; Wilk, L.; Nusair, M. *Can J. Phys.* **1980**, *58*, 1200−1211.
(33) Becke, A. D. *Phys. Rev. A* **1988**, *38*, 3098−3100.
(34) Lee, C. T.; Yang, W. T.; Parr, R. G. *Phys. Rev. B* **1988**, *37*, 785−789.
(35) Michlich, B.; Savin, A.; Stoll, H.; Preuss, H. *Chem. Phys. Lett.* **1989**, *157*, 200−206.
(36) Rosi, M.; Bauschlicher, C. W. *J. Chem. Phys.* **1989**, *90*, 7264−7272.
(37) Trachtman, M.; Markham, G. D.; Glusker, J. P.; George, P.; Bock, C. W. *Inorg. Chem.* **1998**, *37*, 4421−4431.

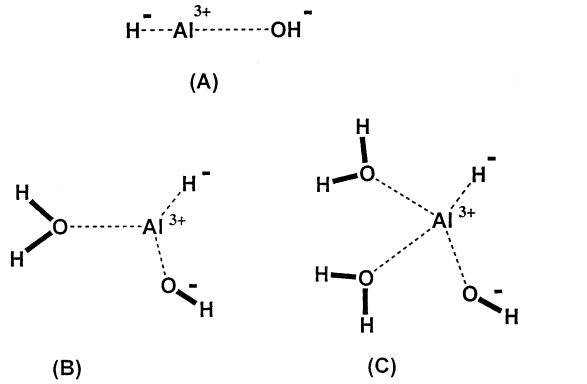

Figure 1. Optimized structures of (A) [H Al(OH)]$^+$, (B) [H Al(OH)-(H_2O)]$^+$, and (C) [H Al(OH)(H_2O)$_2$]$^+$ obtained at the B3LYP/6-31+G** computational level. Bond lengths are in angstroms (Å) and bond angles in degrees (°).

Table 3. Enthalpy Changes, ΔH^o_{298} (kcal/mol), for the Deprotonation Reactions Al[H_2O]$^{n+}$ → Al[OH]$^{(n-1)+}$ + H$^+$ (n = 1−3) Obtained at the B3LYP/6-31+G**//B3LYP/6-31+G** and [B3LYP/6-311++G(3df,3pd)//B3LYP/6-311++G(3df,3pd)] Computational Levels

reaction	ΔH^o_{298}	ΔH^o_{298}
Al[H_2O]$^+$ → Al[OH] + H$^+$	+194.2	[+192.2]
Al[H_2O]$^{2+}$ → Al[OH]$^+$ + H$^+$	+40.2	[+38.8]
Al[H_2O]$^{3+}$ → Al[OH]$^{2+}$ + H$^+$	−118.3	[−119.5]
H_2O → OH^- + H$^+$	+388.0	[+389.9]

latter complexes show significant donor−acceptor stabilization energies for σ interactions involving the occupied in-plane lone-pair Lewis orbital on the water oxygen atom and the empty 3p$_z$ orbital on the aluminum ion, e.g., 14.3 kcal/mol for Al[H_2O]$^+$; these interactions effectively increase the electron density in the Al−O bonding region. Stabilization energies for π-interactions in Al[H_2O]$^{n+}$ (n = 1−3) that transfer charge from the out-of-plane lone-pair 2p$_x$ orbital on the oxygen atom to the 3p$_x$ orbital on the aluminum ion are relatively small but increase from 2.5 kcal/mol in Al[H_2O]$^+$ to 10.1 kcal/mol in Al[H_2O]$^{3+}$. In their computational study of H_2 elimination from large hydrated aluminum clusters with stoichiometry {Al, 20H_2O}$^+$, Reinhard and Niedner-Schatteburg[38] found structures for the inner shell in which the aluminum cation is coordinated through one hydroxide, OH^-, one hydride, H^-, and several H_2O molecules; the overall coordination number of the aluminum ion was 4 or 5. For comparison, we optimized a complex of the form {[H]Al[OH]}$^+$, see Figure 1A. This linear structure is about 10.9 kcal/mol higher in energy than Al[H_2O]$^+$ at the B3LYP/6-311++G(3df,3pd)//B3LYP/6-311++G(3df,3dp) computational level. The NPA charge on the aluminum ion in {[H]Al[OH]}$^+$ is +1.966e, suggesting that its oxidation state is effectively Al^{II}. The hydroxide and hydride ions carry charges of −0.686e and −0.280e, respectively.

Calculated enthalpy changes, ΔH^o_{298} for the deprotonation of Al[H_2O]$^{n+}$ giving Al[OH]$^{(n-1)+}$ + H$^+$ (n = 1−3) are listed in Table 3. The importance of the overall charge on these complexes to the value of ΔH^o_{298} for this process is apparent in this table. The acidity of Al^{3+} solutions, with a

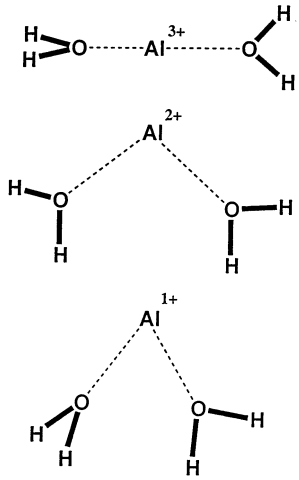

Figure 2. Optimized structures of (A) Al[H_2O]$_2^{3+}$, (B) Al[H_2O]$_2^{2+}$, and (C) Al[H_2O]$_2^{1+}$ obtained at the B3LYP/6-31+G** computational level.

Table 4. Selected Geometrical Parameters and NPA Charges of the Dihydrates Al[H_2O]$_2^{n+}$ (n = 1−3) Calculated at the B3LYP/6-31+G**//B3LYP/6-31+G** Computational Level

dihydrate	geometrical parameters		NPA charges
	Al−O (Å)	∠OAlO (deg)	q_A
Al[H_2O]$_2^{1+}$	2.121	77.5	+0.924e
	2.271		
Al[H_2O]$_2^{2+}$	1.884	103.2	+1.743e
Al[H_2O]$_2^{3+}$ (D_2d)	1.770	180.0	+2.595e

pK of 4.6 for Al[H_2O]$_n^{3+}$ in bulk water, reflects the preponderance of ionized species at neutral pH values.

It should be noted that the structures of Al[OH], Al[OH]$^+$, and Al[OH]$^{2+}$ are all bent,[39] and their Al−O−H angles are 174.7°, 148.6°, and 129.2°, respectively, at the B3LYP/6-311++G(3df,3pd) computational level, see Table 3S. Furthermore, there is a greater transfer of electron density to the aluminum ion for each of the hydroxides than for the corresponding hydrates. These increases (hydroxides vs hydrates) are 13.8%, 8.7%, and 11.3%, respectively, for Al[OH], Al[OH]$^{1+}$, and Al[OH]$^{2+}$ at the B3LYP/6-311++G(3df,3pd) level.

Al[H_2O]$_2^{n+}$ (n = 1−3). Before preceding to the larger aluminum ion complexes, we note that the structures of the dihydrate complexes, Al[H_2O]$_2^{n+}$ (n = 1−3), show some rather interesting variations, see Figure 2. The optimized structure of Al[H_2O]$_2^{3+}$, constrained to have D_{2d} symmetry (angle O−Al−O = 180°), is a local minimum on the B3LYP/6-31+G** PES. The NPA charge on the aluminum ion is about +2.6e, see Table 4, and the NBO analysis of this complex identifies two Al−O dative bonds (0.28*Al + 0.96*O). However, if the optimization is started from an initial structure with one of the two water molecules positioned in the second hydration shell, i.e., Al[H_2O]$^{3+}$•[H_2O], the complex decomposes to Al[OH]$^{2+}$ + H_3O^+, which is significantly lower in energy than the D_{2d} form of Al[H_2O]$_2^{3+}$.

The structure of Al[H_2O]$_2^{2+}$ is bent; the O−Al−O angle is 103.2°. The NBO analysis shows that the additional

(38) Reinhard, R. B.; Niedner-Schatteburg, G. *J. Phys. Chem. A* **2002** *106*, 7988−7992.

(39) Trachtman, M.; Markham, G. D.; Glusker, J. P.; George, P.; Bock, C. W. *Inorg. Chem.* **2001**, *40*, 4230−4241.

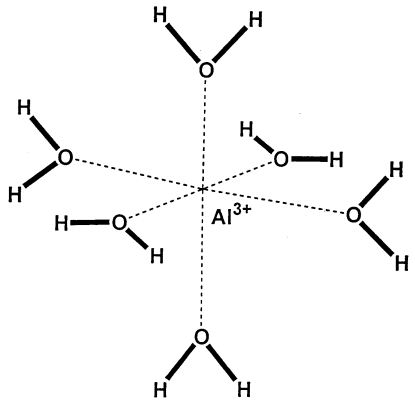

Figure 3. Optimized structure of $Al[H_2O]_6^{3+}$ with T_h symmetry obtained at the B3LYP/6-31+G** computational level.

electron resides primarily in a 3sp hybrid α-orbital on the aluminum ion; no Al−O dative bonds are found in the NBO analysis.

For monovalent aluminum, however, the O−Al−O angle in the optimized structure of $Al[H_2O]_2^{1+}$ is only 77.5°; the Al−O bond lengths are different, 2.12 and 2.27 Å, and the two hydrogen atoms from one of the water molecules are in the O−Al−O plane, whereas the other two hydrogen atoms are on opposite sides of this plane. The NBO analysis of this complex shows the presence of a lone-pair of electrons (which is predominantly in a 3sp hybrid orbital) on the aluminum ion; no Al−O bonds are found among the NBO orbitals. We also considered another point on the $AlO_2H_4^+$ PES in which the aluminum cation is coordinated by one H_2O molecule, one hydroxide, OH^-, and one hydride ion, H^- ($\{Al[H][OH][H_2O]\}^+$, coordination number = 3), see Figure 1B.[38] Interestingly, this complex is 20.2 kcal/mol lower in energy than $Al[H_2O]_2^+$ (coordination number = 2) at the B3LYP/6-311++G(3df,3pd)//B3LYP/6-311++G(3df,3pd) computational level, and the NPA charge on the aluminum cation, +1.874e, suggests that the oxidation state of the aluminum ion is effectively Al^{II}. (For comparison, we show the optimized structure of $\{[H]Al[OH][H_2O]_2\}^+$ in Figure 1C.)

$Al[H_2O]_6^{3+}$, $Al[H_2O]_5^{3+}\cdot[H_2O]$, and $Al[H_2O]_4^{3+}\cdot[H_2O]_2$. We next investigated several hexahydrated trivalent aluminum ion complexes with the six water molecules partitioned between the first and second hydration spheres. Since there are several molecules listed in the CSD that contain an $Al[H_2O]_6^{3+}$ unit, we initially optimized a form of this complex with T_h symmetry,[8,9] see Figure 3, using a variety of methods. The resulting geometrical parameters are listed in Table 5[15,16,32−35] (see also refs 8 and 9). For a given basis set, we find that the Al−O distances obtained from DFT calculations using the hybrid B3LYP method are intermediate between those obtained from the pure DFT methods, LDA (SVWN5) and GGA(BLYP). They are about 0.01 Å longer than those from the corresponding MP2(FULL) method. The NBO analysis of this complex at the B3LYP/6-31+G** computational level finds six Al−O dative bonds (0.23*Al + 0.97*O) that utilize appropriate combinations of the 3s, 3p, and 3d NAOs on the aluminum ion.

Table 5. Geometrical Parameters[a] of the Hexahydrate $Al[H_2O]_6^{3+}$ Calculated at Various Computational Levels

computational level	Al−O (Å)	O−H (Å)	∠HOH (deg)
A. Pure DFT			
Local Density Approximation (LDA)[31]			
SVWN5/6-311++G(d,p)	1.907	0.987	107.5
SVWN5/6-311++G(2d,2p)	1.899	0.985	107.9
SVWN5/6-311++G(3df,3pd)	1.897	0.985	107.5
Generalized Gradient Approximation (GGA)[32−34]			
BLYP/6-311++G(d,p)	1.961	0.985	106.9
BLYP/6-311++G(2d,2p)	1.954	0.983	107.3
BLYP/6-311++G(3df,3pd)	1.952	0.983	107.0
B. Hybrid DFT[15]			
B3LYP/6-31+G(d,p)	1.942	0.978	107.4
B3LYP/6-311++G(d,p)	1.940	0.976	107.1
B3LYP/6-311++G(2d,2p)	1.933	0.973	107.5
B3LYP/6-311++G(3df,3pd)	1.931	0.974	107.2
C. Hartree−Fock (HF)			
HF/6-311++G(d,p)	1.926	0.956	107.3
HF/6-311++G(2d,2p)	1.919	0.954	107.7
HF/6-311++G(3df,3pd)	1.917	0.954	107.4
D. Møller−Plesset Perturbation Theory[16]			
MP2(FULL)/6-311++G(d,p)	1.930	0.973	106.5
MP2(FULL)/6-311++G(2d,2p)	1.921	0.971	107.1

Table 6. Geometrical Parameters and NPA Charges of the Hexahydrates $Al[H_2O]_6^{n+}$ ($n = 1-3$) Calculated at the B3LYP/6-31+G**//B3LYP/6-31+G** [B3LYP/6-311++G(3df,3pd)//B3LYP/6-311++G(3df,3pd)] Computational Level

	geometrical parameters			NPA charges		
hexahydrate	Al−O (Å)	O−H (Å)	∠HOH (deg)	q_{Al}	q_O	q_H
$Al[H_2O]_6^{1+}$ *a*	1.965	0.988	110.6	+0.945e	−1.108e	+0.559e
	[1.944]	[0.984]	[110.1]	[+1.179e]	[−1.070e]	[+0.520e]
$Al[H_2O]_6^{2+}$ *b*	1.967	0.983	109.0	+1.648e	−1.073e	+0.566e
	[1.946]	[0.979]	[108.8]	[+1.544e]	[−0.985e]	[+0.531e]
$Al[H_2O]_6^{3+}$ *c*	1.942	0.978	107.4	+2.076e	−1.063e	+0.609e
	[1.931]	[0.974]	[107.2]	[+1.968e]	[−0.963e]	[+0.568e]

[a] The $Al[H_2O]_6^{1+}$ (T_h) complex is a local minimum on the PES at the HF/6-311++G** computational level, but a sixth-order TS at the B3LYP/6-31+G** and B3LYP/6-311++G(3df,3pd) computational levels. [b] The $Al[H_2O]_6^{2+}$ (T_h) complex is a local minimum on the PES at the HF/6-311++G**, B3LYP/6-31+G**, and B3LYP/6-311++G(3df, 3pd) computational level. [c] The $Al[H_2O]_6^{3+}$ (T_h) complex is a local minimum at the HF/6-311++G**, B3LYP/6-31+G**, and B3LYP/6-311++G(3df, 3pd) computational levels.

The unscaled vibrational frequencies of $Al[H_2O]_6^{3+}$ are listed in Table 4S at the B3LYP/6-31+G** and B3LYP/6-311++G** computational levels. An excellent discussion of the vibrational spectra of this complex can be found in Rudolph et al.[9] along with the calculated frequencies at several other computational levels. A comparison of Al−O breathing frequencies for $Al[H_2O]^{n+}$ and $Al[H_2O]_6^{n+}$ ($n = 1-3$) is given in Table 5S.

For comparison, we optimized structures of $Al[H_2O]_6^{2+}$ and $Al[H_2O]_6^{+}$ with T_h symmetry at the B3LYP/6-31+G** and B3LYP/6-311++G(3df,3pd) computational levels; geometrical parameters and NPA charges for these complexes are listed in Table 6 along with those for $Al[H_2O]_6^{3+}$. The magnitude of the charge transferred from surrounding oxygen atoms to the central aluminum ion in these complexes increases dramatically from ∼0.05e to ∼1.0e as the formal charge on the central aluminum ion increases from +1 to +3. No Al−O bonds are found in the NBO analyses of $Al[H_2O]_6^{2+}$, but there are large stabilization energies associated

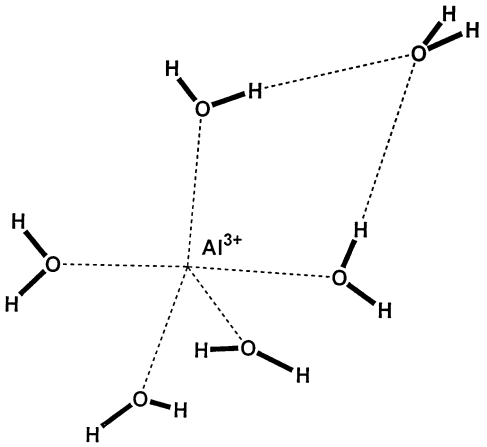

Figure 4. Optimized structure of $Al[H_2O]_5^{2+}\cdot[H_2O]$ obtained at the B3LYP/6-31+G** computational level.

Table 7. Enthalpy Changes, ΔH^o_{298} (kcal/mol), for the Deprotonation $Al[H_2O]_6^{n+} \rightarrow Al[H_2O]_5^{n+}\cdot[OH^-] + H^+$ and Dehydration $Al[H_2O]_6^{n+} \rightarrow Al[H_2O]_5^{n+} + H_2O$ ($n = 2, 3$) Reactions Obtained at the B3LYP/6-31+G**//B3LYP/6-31+G** Computational Level.

reaction	ΔH^o_{298}
$Al[H_2O]_6^{2+} \rightarrow Al[H_2O]_5^{2+}[OH^-] + H^+$	+130.5
$Al[H_2O]_6^{3+} \rightarrow Al[H_2O]_5^{3+}[OH^-] + H^+$	+33.4
$Al[H_2O]_6^{2+} \rightarrow Al[H_2O]_5^{2+} + H_2O$	+14.1
$Al[H_2O]_6^{3+} \rightarrow Al[H_2O]_5^{3+} + H_2O$	+51.8

with donation from the occupied in-plane lone-pair orbital on each of the water oxygen atoms to various vacant 3p orbitals on the aluminum ion. The occupied lone-pair α-orbital on the aluminum ion is primarily a 3s orbital. The monovalent $Al[H_2O]_6^+$ complex with T_h symmetry is not a local minimum on the PES at the B3LYP/6-31+G** or B3LYP/6-311++G(3df,3pd) computational levels.

Enthalpy changes for the deprotonation $Al[H_2O]_6^{n+} \rightarrow Al[H_2O]_5[OH]^{(n-1)+} + H^+$ and dehydration reactions $Al[H_2O]_6^{n+} \rightarrow Al[H_2O]_5^{n+} + H_2O$ ($n = 2, 3$) are listed in Table 7; a few selected geometrical parameters and NPA charges of $Al[H_2O]_5[OH]^{(n-1)+}$ ($n = 2, 3$) are given in Table 6S. It should be noted that the length of the O−H bonds in the aluminum hexahydrates decreases as the formal charge on the aluminum ion increases, which is the reverse of what we find when a single water molecule is present, see Table 2. Dehydration of $Al[H_2O]_6^{3+}$ to $Al[H_2O]_5^{3+} + H_2O$ requires 37.7 kcal/mol more energy than does the corresponding dehydration of the divalent hydrate $Al[H_2O]_6^{2+}$.

Since the coordination number of Al^{3+} in some crystal structures in the CSD is 5, we optimized a hexahydrated trivalent aluminum ion complex with five water molecules initially placed in the first coordination shell and one water molecule in the second shell, positioned to hydrogen bond with two water molecules in the first shell. In the resulting optimized structure of $Al[H_2O]_5^{3+}\cdot[H_2O]$, see Figure 4, the Al−O distance to the water in the second shell is rather short, 3.618 Å at the B3LYP/6-31+G** level, compared to that in the analogous divalent magnesium compound, 3.868 Å.[22] Furthermore, one of the H···O distances involving the second-shell water oxygen atom is extremely short, 1.436 Å compared to 1.802 Å in $Mg[H_2O]_5^{3+}\cdot[H_2O]$, and the O−H distance for the associated inner-shell water is very long, 1.072 Å, suggesting an extremely strong hydrogen bond. Thus, this complex is tending toward $Al[H_2O]_3[OH]^{2+}\cdot[H_3O^+]$. The charge on the aluminum ion, +2.148e, is 0.09e less positive than the charge on the aluminum ion in $Al[H_2O]_6^{3+}$. Interestingly, this complex is only 7.0 kcal/mol higher in energy than $Al[H_2O]_6^{3+}$ at the B3LYP/6-31+G** computational level.

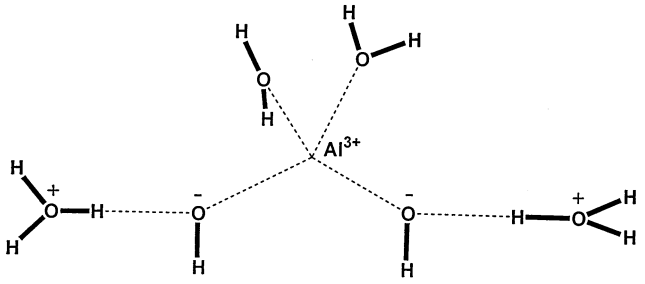

Figure 5. Optimized structure of $Al[H_2O]_2[OH]_2^{+}\cdot[H_3O^+]_2$ obtained at the B3LYP/6-31+G** computational level.

We also optimized a hexahydrated trivalent aluminum ion complex with four water molecules initially placed in the inner coordination shell and two water molecules in the outer shell, each positioned to hydrogen bond to two water molecules in the inner shell. Although the initial structure of this complex could best be described as $Al[H_2O]_4^{3+}\cdot[H_2O]_2$, the resulting optimized structure was better described as $Al[H_2O]_2[OH]_2^{+}\cdot[H_3O^+]_2$; i.e., there have been two proton transfers from water molecules in the first shell to the water molecules in the second shell, see Figure 5. Thus, the coordination number of aluminum remained at 4 during the optimization, but two of the first-shell oxygen atoms are in hydroxide ions rather than water molecules. The Al−O distance to the oxygen atoms of the water molecules in the second shell, 4.124 Å, is much longer than the analogous Al−O distance in $Al[H_2O]_5^{3+}\cdot[H_2O]$, 3.618 Å, or to the corresponding Mg−O distance in $Mg[H_2O]_4^{2+}\cdot[H_2O]_2$, 3.708 Å. The NPA charge on the aluminum ion in this complex is +2.177e, and on each H_3O^+ moiety, the charge is +0.917e. This complex is 11.8 kcal/mol lower in energy than $Al[H_2O]_6^{3+}$ at the B3LYP/6-31+G** computational level. Interestingly, there are no crystal structures in the CSD for 4-coordinate trivalent aluminum species that have 4 water molecules in the inner shell.

$Al[H_2O]_6^{3+}\cdot[H_2O]$. The optimized structure of $Al[H_2O]_6^{3+}\cdot[H_2O]$, in which there is a single water molecule in the second hydration shell, hydrogen bonded to two water molecules in the first hydration shell, is shown in Figure 6. In the absence of second-shell water−water interactions, the dipole moment of the second-shell water molecule is directed toward the central Al^{3+} ion. As shown below, this changes when the second shell is filled with water molecules. The values of ΔH^o_{298} and ΔG^o_{298} for the dehydration reaction

$$Al[H_2O]_6^{3+}\cdot[H_2O] \rightarrow Al[H_2O]_6^{3+} + H_2O$$

are +36.6 and +28.6 kcal/mol, respectively, at the B3LYP/6-31+G** computational level. The value of ΔH^o_{298} for the corresponding dehydration of $Mg[H_2O]_6^{2+}\cdot[H_2O]$ is slightly

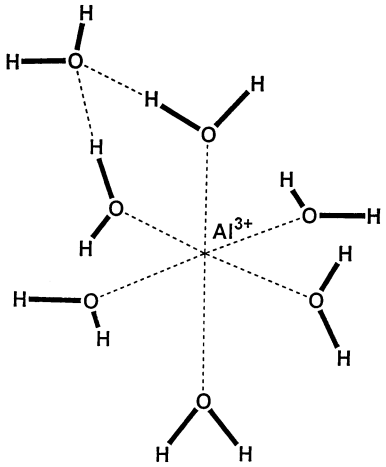

Figure 6. Optimized structure of $Al[H_2O]_6^{3+}\cdot[H_2O]$ obtained at the B3LYP/6-31+G** computational level.

lower, +20.1 kcal/mol, at the B3LYP/6-311++G** level, and the experimental value for the Mg^{2+} complex is +20.3 kcal/mol.[22]

$Al[H_2O]_6^{3+}$ $[H_2O]_{12}$. We considered several models of hydrated Al^{3+} ions with six water molecules in the inner shell, hydrogen bonded to 12 water molecules in the outer shell. Initially, a conformer with T_h symmetry was optimized in which each of the 12 water molecules in the second shell is hydrogen bonded to one of the water molecules in the first shell, but in which there is no hydrogen bonding between water molecules in the second shell, see Figure 7A. Calculations on this form of a metal-ion-complex with a total of 18 water molecules were first reported by Pavlov et al.[40] for Mg^{2+} at the B3LYP/LANL2DZ computational level; we shall refer to this as the PSS(T_h) model. Pye and Rudolph[41] later showed that a fully symmetrized form of this structure was not a local minimum on the HF/6-31G* PES for Mg^{2+}, and we have confirmed their findings at the B3LYP/6-31+G** and B3LYP/6-311++G** computational levels.[22] For Al^{3+}, we find that this PSS(T_h) conformer of $Al[H_2O]_6^{3+}\cdot[H_2O]_{12}$ is a sixth-order transition state at the B3LYP/6-31+G** level, similar to what we found for Mg^{2+}. Thus, dipolar interactions between the 12 second-shell water molecules and the (screened) trivalent aluminum ion are not sufficiently strong to orient the dipole moments of the second-sphere water molecules in a direction toward the central aluminum trication. We note in passing that the presence of the second shell reduces the Al−O distance to the oxygen atom of the first-shell water molecules from 1.942 Å in $Al[H_2O]_6^{3+}$ to 1.917 Å in $Al[H_2O]_6^{3+}\cdot[H_2O]_{12}$; by contrast, the O−H distances increase from 0.978 to 0.994 Å. The distance from Al^{3+} to the second-shell oxygen atoms in this model is 4.183 Å at this computational level, and the distance to all the second-shell hydrogen atoms is 4.821 Å.

We next considered a model with only T symmetry. In this novel model, first proposed by Pye and Rudolph[41] in their study of the second hydration sphere surrounding Mg^{2+},

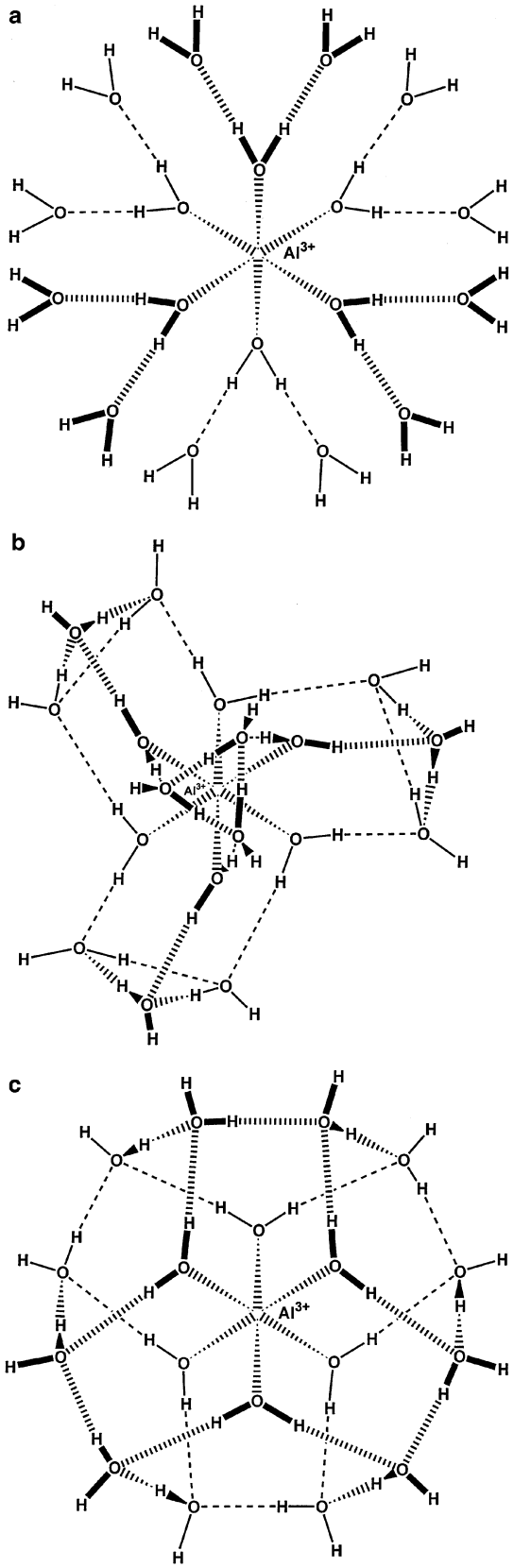

Figure 7. Optimized structures of various models of $Al[H_2O]_6^{3+}\cdot[H_2O]_{12}$: (A) PSS($T_h$), (B) PRC($T$), and (C) MGB($S_6$) obtained at the B3LYP/6-31+G** computational level.

the $Mg[H_2O]_6^{n+}$ unit effectively interacts with four distinct (cyclic) water trimers, see Figure 7B; we shall refer to this as the PRC(T) model. These authors showed that this

(40) Pavlov, M.; Siegbahn, P. E. M.; Sandstrom, M. *J. Phys. Chem. A* **1998**, *102*, 219−228.
(41) Pye, C. C.; Rudolph, W. W. *J. Phys. Chem. A* **1998**, *102*, 9933−9943.

Table 8. Comparison of Total Molecular Energies of the PSS, PRC, and MGB Models of $Al[H_2O]_6^{3+}\cdot[H_2O]_{12}$ and $Mg[H_2O]_6^{2+}\cdot[H_2O]_{12}$ at the B3LYP/6-31+G**//B3LYP/6-31+G** Computational Level

	$Al[H_2O]_6^{3+}\cdot[H_2O]_{12}$		$Mg[H_2O]_6^{2+}\cdot[H_2O]_{12}$	
structure	E_T (au)	ΔE (kcal/mol)	E_T (au)	ΔE (kcal/mol)
PSS (T_h)	−1617.821585[a]	+16.2	−1575.837751[a]	+43.2
PRC (T)	−1617.841576[b]	+3.7	−1575.893395[b]	+8.2
MGB (S_6)	−1617.847464[b]	0.0	−1575.906534[b]	0.0

[a] Sixth-order TS on the B3LYP/6-31+G** PES. [b] Local minimum on the B3LYP/6-31+G** PES.

structure for $Mg[H_2O]_6^{2+}\cdot[H_2O]_{12}$ is a local minimum on the HF/6-31+G* PES, and subsequent optimizations and frequency analyses at the B3LYP/6-31+G** and B3LYP/6-311++G** computational levels have confirmed their results.[22] Rudolph, Mason, and Pye[9] subsequently optimized the analogous form for $Al[H_2O]_6^{3+}\cdot[H_2O]_{12}$ and showed that it was local minimum on the HF/6-31G* PES. We have now reoptimized the PRC(T) form of $Al[H_2O]_6^{3+}\cdot[H_2O]_{12}$ at the B3LYP/6-31+G** computational level and also find it to be a local minimum on the PES, some 12.5 kcal/mol lower in energy than the PSS(T_h) form, see Table 8; the energy difference for the corresponding divalent magnesium complexes is much greater at this computational level, 35.0 kcal/mol.[22] The Al−O distances to the oxygen atoms of the water molecules in the inner shell of this model of $Al[H_2O]_6^{3+}\cdot[H_2O]_{12}$ are 1.922 Å, just slightly longer than those in the PSS(T_h) model; the O−H distances for the inner-shell water molecules are 0.995 Å. The Al−O distances to the oxygen atoms of the water molecules in the second shell are 4.075 Å, about 0.1 Å shorter than for the PSS(T_h) model. It should be noted that, unlike the PSS(T_h) structure, the 24 hydrogen atoms on the water molecules in the second shell fall into two categories: free and hydrogen bonded in one of the four trimers. The corresponding distances from the aluminum ion are significantly different, 4.914 and 4.231 Å, respectively, and the average value 4.572 Å is much less than that found in the PSS(T_h) model.

In order to assess the influence of the charge on the central aluminum ion on the relative energies of the PSS(T_h) and PRC(T) forms, we examined the corresponding structures for Al^{2+} and Al^{+}. Total molecular energies for these forms of $Al[H_2O]_6^{n+}\cdot[H_2O]_{12}$ ($n = 1-3$) are given in Table 7S of the Supporting Information. For each of the three valence states of aluminum, the PRC(T) form is lower in energy than the PSS(T_h) form, and the energy separation decreases as the valence state increases. The PRC(T) form of $Al[H_2O]_6^{2+}\cdot[H_2O]_{12}$ is a local minimum on the PES at the B3LYP/6-31+G** level, and the Al−O and O−H distances for the inner-shell water molecules are very similar to those for the analogous trivalent aluminum complex, 1.922 and 0.994 Å, respectively. The Al···O distances to the second-shell oxygen atoms are 4.088 Å, and the distances to the free and hydrogen bonded second-shell hydrogen atoms are 4.915 and 4.210 Å, respectively. The PSS(T_h) forms of $Al[H_2O]_6^{2+}\cdot[H_2O]_{12}$ and $Al[H_2O]_6^{+}\cdot[H_2O]_{12}$ are not local minima on their respective PESs. Interestingly, the PRC(T) form of $Al[H_2O]_6^{+}\cdot[H_2O]_{12}$ is a local minimum on the PES, even though a form of $Al[H_2O]_6^{+}$ with T_h symmetry, where the outer-shell water molecules are not present, is a sixth-order transition state.

Finally, we considered a model of $Al[H_2O]_6^{3+}\cdot[H_2O]_{12}$ which has only S_6 symmetry, see Figures 7C and 8; no symmetry was actually enforced during the optimization procedure. We first described such a structure in our study of the second hydration shell surrounding divalent magnesium;[22] we shall refer to this as the MGB(S_6) model. This form of $Al[H_2O]_6^{3+}\cdot[H_2O]_{12}$ has a more integrated hydrogen bonded network than that of the PRC(T) structure. It is apparent from Figure 7C that the main structural units of the water molecules in this model of $Al[H_2O]_6^{3+}\cdot[H_2O]_{12}$ are (cyclic) pentamers constructed from four second-shell water molecules and one first-shell water molecule. It should be noted, however, that the structure of these pentamers is somewhat different from the structure of the cyclic global minimum on the PES of $[H_2O]_5$, for which one hydrogen atom from each water molecule is not involved in a hydrogen bond. For the pentamers in our form of $Al[H_2O]_6^{3+}\cdot[H_2O]_{12}$, both hydrogen atoms from the inner-shell water molecule are hydrogen bonded in the same pentagonal ring. Furthermore, neither of the hydrogen atoms from one of the four water molecules in the second shell is hydrogen bonded in the same ring, see Figure 7C. (The energy difference between a pentamer at its geometry in $Mg[H_2O]_6^{2+}\cdot[H_2O]_{12}$ and a fully optimized cyclic water pentamer is substantial, 19.2 kcal/mol at the B3LYP/6-31+G** level.[22]) Our model of $Al[H_2O]_6^{3+}\cdot[H_2O]_{12}$ has a "sandwichlike" structure, similar to that found by Glendening et al.[42] and Kim et al.[43] for the inner-shell water molecules of $Na[H_2O]_6^{+}$, in which the cation−water interactions are relatively weak.

Frequency analyses confirm that this MGB(S_6) form of $Al[H_2O]_6^{3+}\cdot[H_2O]_{12}$ is a local minimum on the PES at the B3LYP/6-31+G**//B3LYP/6-31+G** computational level; it is, however, only 3.7 kcal/mol lower in energy than the PRC(T) model, see Table 8. The energy difference for the corresponding divalent magnesium conformers is more than double this value (8.2 kcal/mol at this computational level). In Table 8S, we provide various structural parameters for this model and compare them with the analogous values for the corresponding form of the divalent magnesium complex.[22] The average Al−O and O−H distances for the inner-shell water molecules for the MGB(S_6) form of $Al[H_2O]_6^{3+}\cdot[H_2O]_{12}$ are 1.922 and 0.994 Å, respectively, which are essentially the same as those for the PRC(T) form; the average Mg−O distance for the inner-shell water molecules in the corresponding form of $Mg[H_2O]_6^{2+}\cdot[H_2O]_{12}$ is considerably longer, 2.098 Å. The average Al···O distances to the water molecules in the second shell of the MGB(S_6) form of the 18 water complex is 3.962 Å, some 0.1 Å shorter than we found for the PRC(T) model, and nearly 0.17 Å shorter than the average Mg···O distance in the analogous divalent magnesium complex. The average distance from the aluminum ion to the 12 free second-shell hydrogen atoms is

(42) Glendening, E. D.; Feller, D. *J. Phys. Chem.* **1995**, *99*, 3060−3067.
(43) Kim, J.; Lee, S.; Cho, S. J.; Mhin, B. J.; Kim, K. S. *J. Chem. Phys.* **1995**, 839−849.

Table 9. Calculated NPA Charges for $Al[H_2O]_6^{3+}$ (T_h), $Al[H_2O]_6^{3+}\cdot[H_2O]_{12}$ (T_h, PSS), $Al[H_2O]_6^{3+}\cdot[H_2O]_{12}$ (T, PRC), and $Al[H_2O]_6^{3+}\cdot[H_2O]_{12}$ (S_6, MGB) Obtained at the B3LYP/6-31G**//B3LYP/6-31+G** Computational Level

	NPA charges				
	aluminum ion	inner shell		outer shell	
complex	q_{Al}	Σq_O	Σq_H	Σq_O	Σq_H
$Al[H_2O]_6^{3+}$ (T_h)	+2.058e	−6.230e (+0.942e)	+7.172e	-	-
$Al[H_2O]_6^{3+}\cdot[H_2O]_{12}$ (PSS(T_h))	+2.020e	−6.401e (+0.247e)	+6.648e	−11.798e (+0.733e)	+12.531e
$Al[H_2O]_6^{3+}\cdot[H_2O]_{12}$ (PRC(T))	+2.028e	−6.414e (+0.228e)	+6.642e	−12.103e (+0.744e)	+12.847e
$Al[H_2O]_6^{3+}\cdot[H_2O]_{12}$ (MGB(S_6))	+2.037e	−6.397e (+0.202)	+6.599e	−12.137e (+0.760e)	+12.897e

Table 10. Aluminum Coordination in Crystal Structures in the CSD: Number of Structures[a]

Inner Sphere			
ligands	CN 4	CN 5	CN 6
O, N, S, Cl, Br	419	61	130
O, N, S	148	33	109
O only	96	14	63
N only	38	3	11
S only	0	0	1

Number of Inner-Sphere Water Molecules				
	1 H_2O	2 H_2O	3 H_2O	6 H_2O
CN 4		none		
CN 5	1			
CN 6	9	10	1	7

[a] CSD, April 2001 version. CN = coordination number.

4.846 Å, while the distance to the 12 second-shell hydrogen atoms involved in hydrogen bonds is only 4.095 Å at the B3LYP/6-31+G** level. It should be noted, however, that no splitting of the second peak of the Al−H radial distribution function was observed in molecular dynamics studies of Al^{3+} in solution.[10] This difference may be a consequence of the isolated nature of our cluster.

When the second coordination shell is included with the additional 12 water molecules, the NPA charge on the aluminum ion is slightly less positive than that of $Al[H_2O]_6^{3+}$ for each of the models, see Table 9. The remaining positive charge resides primarily on the outer coordination shell in all three models, showing that the second shell water molecules donate more than 0.7e to $Al[H_2O]_6^{3+}$.

The unscaled vibrational frequencies of the MGB(S_6) form of $Al[H_2O]_6^{3+}\cdot[H_2O]_{12}$ at the B3LYP/6-31+G** computational level are listed in Table 9S of the Supporting Information. A comparison of Al−O breathing vibrations for several aluminum complexes with different charges are given in Table 5S of the Supporting Information. For both the PRC(T) and MGB(S_6) models of $Al[H_2O]_6^{3+}\cdot[H_2O]_{12}$, the Al−O breathing frequency is greater than that for an isolated $Al[H_2O]_6^{3+}$ complex.

CSD Analysis. Crystal structures, those done either by X-ray or by neutron diffraction, containing aluminum and O, N, S, Cl, and/or Br were extracted from the CSD. The results are shown in Table 10. There were 130 structures with coordination number 6, 61 with coordination number 5, and 419 with coordination number 4. Apparently, coordination number 4 is strongly preferred among these structures. Among the 130 structures in which aluminum has a coordination number of 6, there were 9 in which the aluminum ion was hexahydrated. Interestingly, none of the structures with coordination number 4 contained four water molecules in the inner shell. Only one of the coordination number 5 structures contained any water molecules, and even then, there was only one. When the coordination-number analysis was repeated for structures containing only O, N, or S bound to the aluminum, coordination numbers 4 and 6 were more similar in number (see Table 10). Numbers of structures in which all atoms in the innermost sphere are the same (O, N, or S) are also listed in this table.

Consistent with the crystallographic data, DFT calculations show that a hexacoordinated trivalent aluminum ion with all six water molecules in the first coordination shell, $Al[H_2O]_6^{3+}$ (T_h), is lower in energy than a structure with five water molecules in the first shell plus one in the second shell that is hydrogen bonded to water molecules in the first shell, $Al[H_2O]_5^{3+}\cdot[H_2O]$. As noted previously, we were not able to find a local minimum on the PES that could be described as having four water molecules in the first shell and two in the second shell, e.g., $Al[H_2O]_4^{3+}\cdot[H_2O]_2$. Although this optimization was started using the geometry of $Mg[H_2O]_4^{2+}\cdot[H_2O]_2$, two internal proton transfers took place during the optimization giving $Al[H_2O]_2[OH]_2^{+}\cdot[H_3O^+]_2$; this structure is nearly 5 kcal/mol lower in energy than $Al[H_2O]_6^{3+}$ at the B3LYP/6-31+G** computational level.

Aluminum does not play a significant role in protein structures deposited in the Protein Data Bank. It has mainly been used as the trifluoride, AlF_3, to mimic the planar PO_3 entity in the transition state of phosphoryl transfer reactions.[44−50] In each case, the planar AlF_3 is found in a trigonal bipyramidal complex in which the aluminum is positioned between two axially oriented oxygen atoms, one from a phosphate group. There were no aluminum−protein interac-

(44) Sondek, J.; Lambright, D. G.; Noel, J. P.; Hamm, H. E.; Sigler, P. B. *Nature* **1994**, *372*, 276−279.
(45) Scheffzek, K.; Ahmadian, M. R.; Kabsch, W.; Wiesmüller, L.; Lautwein, A.; Schmitz, F.; Wittinghofer, A. *Science* **1997**, *277*, 333−338.
(46) Schlichting, I.; Reinstein, J. *Nat. Struct. Biol.* **1999**, *6*, 721−723.
(47) Sudom, A. M.; Prasad, L.; Goldie, H.; Delbaere, L. T. J. *J. Mol. Biol.* **2001**, *314*, 83−92.
(48) Madhusudan; Akamine, P.; Xuong, N.-H.; Taylor, S. S. *Nat. Struct. Biol.* **2002**, *9*, 273−277.
(49) Wang, W.; Cho, H. S.; Kim, R.; Jancarik, J.; Yokota, H.; Nguyen, H. H.; Grigoriev, I. V.; Wimmer, D. E.; Kim, S.-H. *J. Mol. Biol.* **2002**, *319*, 421−431.
(50) Collyer, C. A.; Henrick, K.; Blow, D. M. *J. Mol. Biol.* **1990**, *212*, 211−235.

Table 11. Neutron Diffraction Data on Aluminum Hydrates

CSD refcode or chemical formula	Al−O distance (Å)	inner sphere	*X*−O−Al angle (deg)[a]	Al−second sphere O or Cl	second sphere	refs
MAMALM 02	6 × 1.850	6 H_2O	6 × 163.88	6 × 4.068 6 × 4 0.633	6 sulfate O 6 2nd sphere H_2O	24
SOGGEA	2 × 1.872 2 × 1.881 1.918 1.885	6 H_2O	2 × 180.00 2 × 164.22 2 × 174.37	2 × 4.061, 4.160 2 × 4.057, 4.216 2 × 4.303, 3.862	12 carboxylate O	25
TAPBOB 06	1.878, 1.889 1.906, 1.876 1.853, 1.918	6 H_2O	168.433, 170.45 153.403, 155.80 165.130, 162.58	3.986, 4.014 3.918, 3.926 4.101, 3.854 3.826, 4.048 3.934, 4.109 4.120, 3.939	12 sulfate O	26
$AlCl_3 \cdot 6H_2O$	6 × 1.883	6 H_2O	6 × 172.635	6 × 4.350 6 × 4.488	12 chloride	28, 29
average	1.876		168.0	4.052 O 4.419 Cl		

[a] *X* is halfway between the two hydrogen atoms of water molecules bound directly to the aluminum ion.

tions in these macromolecular structures. There is one example of an enzyme in which the native metal ion has been replaced by aluminum.[50] The aluminum ion in this structure is hexacoordinated. A second site, described in the article as filled by a magnesium ion, is also hexacoordinated. As the electron count in Al^{3+} and Mg^{2+} is the same (i.e., 10), the assignment of which metal ion is which, or whether each site is a mixture, must await further study, such as neutron diffraction.

Neutron Crystallography Results. Four crystal structures of aluminum complexes studied by neutron diffraction are listed in Table 11.[24−29] Interestingly, they all contain a central $Al[H_2O]_6^{3+}$ unit with Al−O distances in the range 1.85−1.92 Å (average 1.876 Å). The deviations of the plane of the water molecules from the O−Al^{3+} vector (calculated by setting a point *X* halfway between the two hydrogen atoms) vary from 27° to 0° with an average value of 12°. The second shell consists of oxygen atoms (from carboxylate, sulfate or second-sphere water molecules) at an average distance of 4.05 Å, or chloride ions at an average of 4.42 Å. This outer shell is where anions accumulate in the crystal structures. The presence of anions in the second coordination sphere of the aluminum ions makes it difficult to compare the neutron diffraction results of the geometry of the inner $Al[H_2O]_6^{3+}$ core with that of our model, $Al[H_2O]_6^{3+} \cdot [H_2O]_{12}$.

Concluding Remarks. DFT calculations show that a hexahydrated trivalent aluminum ion with all six water molecules in the first coordination shell, $Al[H_2O]_6^{3+}$ (T_h), is lower in energy than a structure with five water molecules in the first shell and one in the second shell, that is hydrogen bonded to water molecules in the first shell, $Al[H_2O]_5^{3+} \cdot [H_2O]$. However, we were not able to find a local minimum on the PES that could be described as having four water molecules in the first shell and two in the second shell, e.g., $Al[H_2O]_4^{3+} \cdot [H_2O]_2$. Two internal proton transfers took place during the optimization giving a structure of the form $Al[H_2O]_2[OH]_2^{+} \cdot [H_3O^+]_2$, which is nearly 5 kcal/mol lower in energy than $Al[H_2O]_6^{3+}$ at the B3LYP/6-31+G** computational level.

Multiple water molecules in the second hydration shell of a metal cation present the option of intricate hydrogen bonding networks that can help stabilize the resulting complex. For example, the successive addition of water stabilizes $Al[H_2O]_n^{3+} \cdot [H_2O]$ complexes from the proton transfers that lead to an OH^- in the inner shell and an H_3O^+ in the outer shell. These ionizations, which are well-known in the experimental literature of Al^{3+}, are not seen with Mg^{2+} at similar hydration numbers (indicative of the higher pK_a values for divalent than trivalent metal ions[51−53]), and this may account for the lack of usage of aluminum (or other trivalent cations) in enzyme reactions; their effects on ligand ionization may be too extreme to be tolerated.

Rudolph, Mason, and Pye[9] discovered the first true local minimum on the HF/6-31G* PES of $Al[H_2O]_6^{3+} \cdot [H_2O]_{12}$, and our higher-level DFT calculations, which include electron correlation, find that this structure is also a local minimum on the B3LYP/6-31+G** PES. This novel structure has *T* symmetry, and the 12 second-sphere water molecules are grouped into four water trimers attached to an octahedral $Al[H_2O]_6^{3+}$ moiety. We have now identified a lower-energy local minimum on the B3LYP/6-31+G** PES of $Al[H_2O]_6^{2+} \cdot [H_2O]_{12}$. This new minimum, which has only S_6 symmetry, has a more integrated hydrogen bonded network than the structure proposed by Rudolph, Mason, and Pye,[9] and it is 3.7 kcal/mol lower in energy. Our calculations, in accord with those of Rudolph, Mason, and Pye,[9] suggest that the interactions between the 12 second-shell water molecules (Al···O > 3.99 Å) and the trivalent aluminum ion in $Al[H_2O]_6^{3+} \cdot [H_2O]_{12}$ are not sufficiently strong to orient the dipole moments of these second-shell water molecules in a direction toward the central aluminum ion.

We cannot, of course, claim from these calculations that the MGB(S_6) structure of $Al[H_2O]_6^{3+} \cdot [H_2O]_{12}$ is the global minimum on the PES, but it is currently the lowest-energy

(51) George, P.; Trachtman, M.; Bock, C. W.; Glusker, J. P. *Chem. Phys. Lett.* **2002**, *351*, 454−458.
(52) Rustad, J. R.; Dixon, D. D.; Russo, K. M.; Felmy, A. R. *J. Am. Chem. Soc.* **1999**, *121*, 3234−3235.
(53) Brown, P. L.; Sylva, R. N.; Ellis, J. *J. Chem. Soc., Dalton Trans.* **1985**, *4*, 723−730.

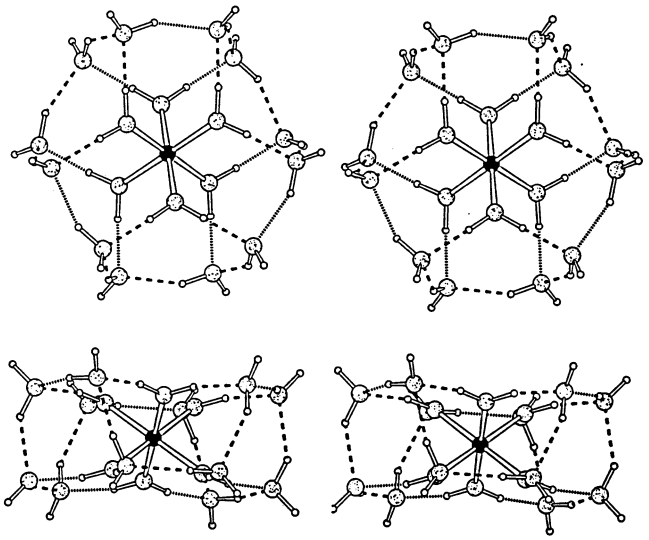

Figure 8. Stereoviews of two aspects of the MGB(S_6) model of $Al[H_2O]_6^{3+}\cdot[H_2O]_{12}$

form that is known. Furthermore, the arrangement of the 18 water molecules surrounding the Al^{3+} ion in this form of $Al[H_2O]_6^{3+}\cdot[H_2O]_{12}$ is consistent with the structural data in the crystallographic literature. The geometry of the hydrogen bonded network in our structure contains pentameric clusters composed of four water molecules from the second shell and one from the first shell. Water pentamers are thought to be common in pure water, and thus, the second shell appears to provide a smooth transition between the ligation sphere of Al^{3+} and bulk solvent. The fact that the second shell has so many surface hydrogen bonds no doubt contributes to the aggregation of more water molecules on that surface, providing the connectivity to bulk water. In other words, the hydrogen bonds with the second hydration shell enable the third hydration shell to approach the structure of bulk water.

The presence of a second solvation sphere surrounding Al^{3+} decreases the net charge on the aluminum ion compared to its value in $Al[H_2O]_6^{3+}$ (+2.058e). This is true whether the PRC(T) form (+2.028e) or the MGB(S_6) form (+2.037e) of the hydrogen bonded network is used for the calculation; similar results have been reported for the divalent magnesium complexes. The main effect of the second hydration sphere surrounding Al^{3+}, however, is on the water molecules in the first hydration shell; their net charge is changed from +0.94e in $Al[H_2O]_6^{3+}$ to only about +0.20e in $Al[H_2O]_6^{3+}\cdot[H_2O]_{12}$. In addition, the second hydration sphere surrounding either Al^{3+} or Mg^{2+} reduces the metal−oxygen distances to the six water molecules in the inner shell for both the PRC(T) and MGB(S_6) forms of the 18 water complexes.

A comparison of our model structure of $Al[H_2O]_6^{3+}\cdot[H_2O]_{12}$ (Figures 7C and 8) with a regular dodecahedron of water molecules shows that the two structures are remarkably similar, see Figure 9. The main difference is that six of the water molecules of the dodecahedron lie in the first, rather than second, coordination shell of water molecules. This leaves sites for the binding of water at 14 out of the 20 vertexes of the water dodecahedron in the second shell. But only 12 of these 14 are hydrogen bonded to the six water

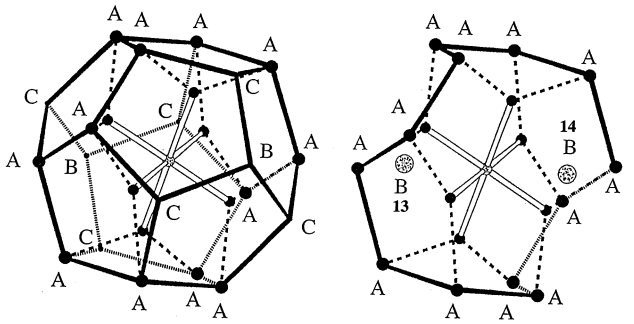

Figure 9. Relationship of the MGB(S_6) model with $Al[H_2O]_6^{3+}\cdot[H_2O]_{12}$ to a pentagonal dodecahedron. Shown on the left is a regular dodecahedran with $Al[H_2O]_6^{3+}$ inserted in its center. Vertexes A are occupied by water molecules hydrogen bonded to inner-shell water molecules attached to the aluminum ion. Vertexes C are empty; they are too close to Al^{3+}-bound water molecules. Vertexes B are two additional bonding sites. The actual model (A and B vertexes) is shown on the right.

molecules of the inner coordination shell. Two positions (13th and 14th coordination positions) are left unoccupied, and as a result, the model is not spherically symmetric but somewhat flat (as seen in Figure 8B). Presumably, the locations of these 13th and 14th coordination positions vary dynamically. These two additional (13th and 14th) positions associated with the MGB(S_6) form of the $Al[H_2O]_6^{3+}\cdot[H_2O]_{12}$ complex may be available to bind additional water molecules, possibly leading to a coordination number of 14 rather than 12 in the second hydration shell. These two ligands are, however, differently bonded and more weakly held than the other 12 ligands which are directly hydrogen bonded to water molecules in the first hydration shell. The presence of these additional (although more weakly bound) ligands might account for the second-shell hydration number of 14 found by molecular dynamics.[10]

Acknowledgment. This work was supported by National Institutes of Health, Grants GM31186, CA10925, CA06927, and was also supported by an appropriation from the Commonwealth of Pennsylvania. We thank the Advanced Scientific Computing Laboratory, NCI-FCRF, for providing time on the Cray YMP and J90 computers. The authors would also like to thank Dr. Cory Pye for providing coordinates for his 18 water complexes and Carol E. Afshar for technical assistance. The contents of this manuscript are solely the responsibility of the authors and do not necessarily represent the official views of the National Cancer Institute, or any other sponsoring organization.

Supporting Information Available: Tables of calculated values of E (Table 1S), Σ, S, and C_v (Table 2S); the geometrical parameters and NPA charges of $Al[OH]^{(n-1)+}$ ($n = 1-3$) (Table 3S); vibrational frequencies of $Al[H_2O]_6^{3+}$ (Table 4S); Al−O breathing frequencies (Table 5S); selected geometrical parameters and NPA charges of $Al[H_2O]_5[OH]^{(n-1)+}$ ($n = 2, 3$) (Table 6S); E of different forms of $Al[H_2O]_6^{n+}\cdot[H_2O]_{12}$ ($n = 1-3$) (Table 7S); M−O and M−H distances in the divalent magnesium and trivalent aluminum MGB-(S_6) complexes (Table 8S); and vibrational frequencies of trivalent aluminum MGB(S_6) complex (Table 9S). This material is available free of charge via the Internet at http://pubs.acs.org.

IC020602E